

Aqueous- and Solid-Phase Biogeochemistry of a Calcareous Aquifer System Downgradient from a Municipal Solid Waste Landfill (Winterthur, Switzerland)

ARIA AMIRBAHMAN,*
RENÉ SCHÖNENBERGER,
C. ANNETTE JOHNSON, AND LAURA SIGG
*Swiss Federal Institute of Environmental Science and
Technology (EAWAG) and Swiss Federal Institute of
Technology, (ETHZ), Zürich, Switzerland*

This study addresses the biogeochemical changes that take place in a calcareous aquifer system under and downgradient from a municipal solid waste landfill. Aqueous-phase chemical analysis of the redox-sensitive species indicates the presence of aerobic respiration, denitrification/ NO_3^- reduction, and Fe(III), Mn(III/IV), and SO_4 reduction processes under the landfill. Because available and released organic matter is limited, reduction processes downgradient from the landfill do not go far beyond aerobic respiration, denitrification, and Mn(III/IV) reduction. Assuming steady-state conditions, STEADYQL computer program has been used to model the biogeochemical processes by taking into account the kinetics of the redox reactions, calcite precipitation and dilution. Dilution has the most significant influence on the concentrations of the dissolved organic and inorganic carbon. Dissolved Mn(II) concentrations in the entire anaerobic zone are controlled by the solubility of rhodocrocite [$\text{MnCO}_3(\text{S})$]. At selected locations under the landfill where SO_4 reduction takes place, dissolved Fe(II) concentrations are regulated by the solubility of amorphous FeS. Chemical extraction of the aquifer solid phase indicates that the oxidation capacity of this aquifer system is largely controlled by iron(III) (hydr)oxides. Due to Fe(III)-reducing processes, the concentration of iron(III) (hydr)oxides has diminished under the landfill. Downgradient along the leachate plume, where no Fe(III)-reducing processes are currently observed, decreased concentrations of solid Fe(III) phases and the presence of iron(II) sulfide phases suggest that, in the past, Fe(III)- and SO_4 -reducing processes have indeed taken place. This is presumably due to the presence of higher concentrations of available organic matter in the past.

Introduction

The presence of high concentrations of dissolved organic carbon (DOC) in an aquifer system can result in the development of a reducing zone due to microbial activity. These conditions are frequently found along landfill leachate

plumes, where zones of microbially catalyzed redox reactions are usually observed (1). Geochemical changes that occur in an aquifer downgradient from the infiltration of water with a high DOC concentration may have significant consequences on the quality of groundwater. Such changes are influenced by mass- and electron-transfer processes that are directly or indirectly connected with the microbial degradation of DOC (2–4). Therefore, understanding the processes that control the fate of organic matter and other redox-sensitive parameters is essential in assessing the extent of groundwater pollution and designing remedial measures.

In this paper, we present the results of the aqueous- and solid-phase chemical analysis of a calcareous aquifer system under and downgradient from a municipal solid waste landfill. We have taken a quantitative approach to characterize the biogeochemical processes along the leachate plume. The computer program STEADYQL (5) has been used to quantify and compare the influence of the microbially catalyzed redox processes, calcite precipitation, and dilution on the geochemical changes downgradient from the landfill. Analysis of the solid Fe phases has been conducted to assess the long-term impact of the presence of the landfill on the aquifer.

Experimental Section

Site Description. The site, landfill Riet, is located at the city of Winterthur in Switzerland (Figure 1). The landfill under study, landfill I, is unlined and was used between 1950 and 1963, after which it was capped with a layer of humus. It contains ca. 50 000 m^3 of household and demolition waste. Landfill II was filled between 1918 and 1924. Currently, the land above landfills I and II is used for agricultural purposes. The aquifer to the southeast of these landfills is oxic, and to the northwest, there are more solid waste landfills filled during the period between 1925 and the present (Figure 1). The sediment is lithologically and texturally variable and is characterized by an unconsolidated quaternary glacial/fluvial deposit consisting of CaCO_3 (40–60%) and silicate minerals.

Wells number 1, 2, 20, and 21 were drilled under landfill I (Figure 1). Wells 22 and 23 are situated under landfill II, and wells 3–6 are in the oxic part of the aquifer. Hydrological modeling of this site has shown that the groundwater flows from landfill I to the direction of wells 22 and 23 with an average velocity of 30 cm day^{-1} under landfill II (6). Downgradient from well 23, due to the presence of man-made obstacles, no further wells were drilled.

Field Sampling. Aqueous samples were collected from the wells by pumps. Approximately two well volumes were pumped before samples were collected into acid-washed HDPE bottles. All of the samples were filtered through pre-washed 0.45 μm cellulose nitrate filters. Dissolved metal and S(-II) samples were filtered into 0.1 M HNO_3 and 0.1 M Zinc acetate solutions in the field, respectively. All of the samples were stored in the dark at 4 °C and were analyzed less than 24 h after collection. Details of aqueous sampling procedure are given elsewhere (7).

Solid-phase-sampling technique is described elsewhere (8). Samples were collected in 2 m long plastic or Plexiglas bore core liners with a 10 cm inner diameter. The headspace at the two ends of the liners was purged with Ar gas, and the liners were capped. To minimize the extent of O_2 contamination, the cores were wrapped with Saran foils and transferred to Teflon bags. After purging with Ar, the Teflon bags were heat-sealed at the end. In the laboratory, the cores were frozen, cut into 30 cm pieces and transferred to an anaerobic glovebag (Coy Lab. Products, Inc., Grass Lake, MI),

* Corresponding author present address: Department of Civil and Environmental Engineering, 5706 Aubert Hall, University of Maine, Orono, ME 04473. Phone: (207)581-1277; fax: (207)581-3888; e-mail: aria@umit.maine.edu.

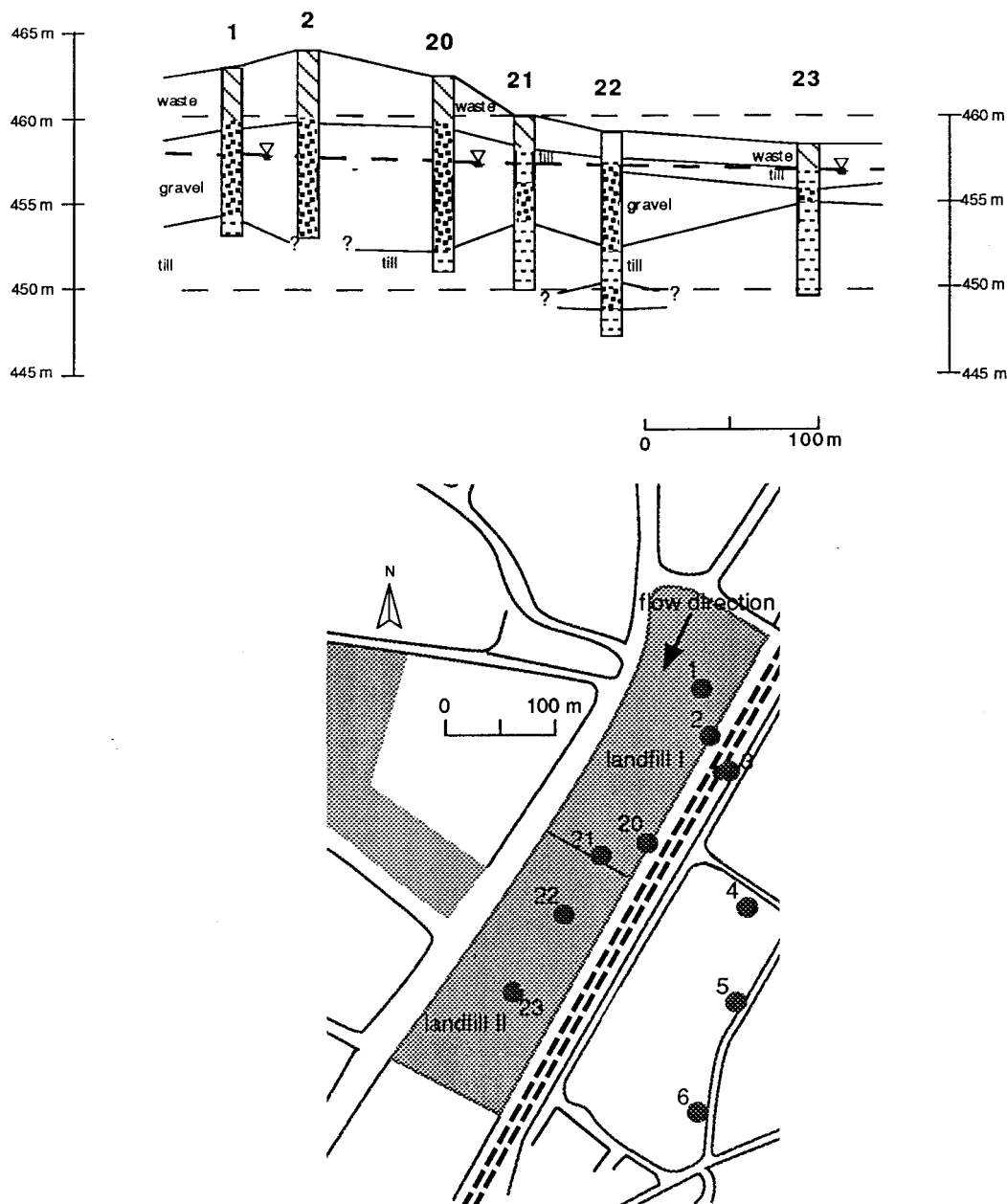


FIGURE 1. Landfill Riet profile and plan, indicating the location of the wells and the flow direction.

TABLE 1. Chemical Composition of the Groundwater^a

well	DOC	Cl ⁻	H ₃ BO ₃	SO ₄ ^b	NO ₃ ⁻	DIC ^b	Na ⁺	Ca ^b	Mg ^b	S(-II) _{aq} ^b	Fe(II) ^b	Mn(II) ^b	NH ₄ ⁺	O ₂ (aq)	pH	temp	conductivity
1	15.4	890	66.0	560	21	22 500	1280	5000	3540	2.96	284	20	1810	≤6	6.84	11.3	2140
20	8.4	430	30.4	650	240	15 100	1510	5610	1960	0.90	44	19	322	≤6	6.74	11.0	1548
21	13.0	360	21.6	1070	20	15 200	260	6920	1220	1.56	585	18	426	≤6	6.71	10.2	1606
22	5.3	150	12.5	780	180	11 000	240	5020	1000	≤0.1	3.1	20	19	≤6	6.76	8.5	1134
23	2.3	770	7.35	650	360	8800	740	3900	1000	≤0.1	0.45	10	32	≤6	6.90	8.1	1035
oxic	1.2	460	1.82	250	650	7100	370	3580	1120	≤0.1	≤0.05	≤0.01	≤0.5	188	7.02	8.0	750

^a All concentrations other than DOC are expressed (μM). The DOC concentration is in parts per million. Temperature and conductivity are reported (°C and μS cm⁻¹, respectively). ^b Total concentrations in the aqueous phase.

where they were stored for no longer than 1 month. All of the analyses were performed during that period. The chemical extractions of the samples were conducted only using the middle 10 cm of each core.

Aqueous-Phase Chemical Analysis. The analyzed chemical species in the groundwater samples are listed in Table 1. The DOC concentration was measured with a TOC-5000A instrument (Shimadzu). Measurement of alkalinity was

performed by titration with a standardized 0.01 M HCl solution. Values of alkalinity were converted to dissolved inorganic carbon (DIC) concentrations. Concentrations of Cl⁻, SO₄ and NO₃⁻ were measured by ion chromatography (Dionex) using an AS11 anion-exchange column. Dissolved Mn(II), Fe(II), Na⁺, K⁺, Ca, Mg, and H₃BO₃ (borate) were measured using ICP-AES (Spectro Analytical Instruments). Dissolved O₂, conductivity, pH, and temperature were

determined in situ by a combined LF-196 instrument (WTW, Wellheim, Germany). Dissolved S(-II) concentrations were measured by photometric analysis using methylene blue (9). Flow injection analysis (Procon, Switzerland) was used to determine NH_4^+ .

Solid-Phase Chemical Analysis. The solid-phase samples were analyzed using chemical extraction techniques. Identification of various Fe phases was the primary goal of these extractions.

Due to the presence of a high amount of Fe(II) within the calcite deposits, HCl extraction methods commonly used to distinguish between amorphous and crystalline Fe(III) phases in sandy aquifers (10) rendered very high concentrations of Fe(II), and therefore, were not used to characterize the Fe(III) phases. To determine the concentration of the available iron(III) (hydr)oxides, reductive dissolution techniques were employed. Relative to the acid extraction methods, the reductive methods do not significantly dissolve the calcite deposits.

The concentration of the available amorphous iron(III) (hydr)oxides was determined by ascorbate extraction at pH 8 (11). Briefly, ca. 1 g of wet sediment was added to 20 mL of a 0.12 M sodium ascorbate, 0.17 M sodium citrate, and 0.6 M NaHCO_3 solution. The suspensions were shaken in the anaerobic glovebag in the dark for 24 h and then filtered. The Fe concentrations were measured by atomic absorption spectrometry (AAS, Perkin-Elmer 5000). The data reported here are corrected by subtracting the blank Fe concentrations from similar extractions with a solution of 0.17 M sodium citrate and 0.6 M NaHCO_3 only. Experiments with synthetic iron(III) (hydr)oxides showed that nearly all of amorphous hydrous ferric oxide (HFO) and less than 2% of lepidocrocite and goethite was extracted by ascorbate at pH 8.

The Ti(III)-EDTA extraction technique was used to estimate the operationally defined oxidation capacity (OXC) (12). Extractions were conducted by adding ca. 1 g of wet solid sample to a 20 mL solution of 8 mM Ti(III) dissolved in 50 mM EDTA at a near-neutral pH. The samples were shaken in the dark for 24 h and filtered in the anaerobic glovebag. The OXC was determined by the photometric measurement of the concentration of unreacted Ti(III) at 550 nm.

In this work, Ti(III)-EDTA/extractable Fe(III) is used as an indicator for the total reducible Fe(III) phases (12). The reported concentrations are corrected for the background concentrations after conducting blank experiments with the sample in a 50 mM EDTA solution only. Ti(III)-EDTA extractions of synthetic iron(III) (hydr)oxides showed that HFO and lepidocrocite were completely, and hematite and goethite were more than 90%, reduced. With this technique, however, only 5% of magnetite can be extracted (10).

Acid volatile sulfide (AVS) consisting primarily of amorphous FeS was measured by boiling ca. 1 g of sediment in a 20 mL solution of 6 M HCl for 1 h in an enclosed vessel. The released H_2S was transported by a stream of N_2 gas, trapped in a 40 mL solution of 0.1 M zinc acetate and measured photometrically (9). Organic and elemental sulfur [S(0)] were determined by adding a 20 mL solution of acetone to the residue sediment from the AVS measurements and boiling for ca. 16 h (9). Total reducible sulfur was extracted by a 40 mL solution of 1 M Cr(II) dissolved in 0.5 M HCl at the boiling temperature for 1.5 h (13). Measurement was done after trapping sulfide in a zinc acetate solution as above.

Geochemical Modeling. The computer program STEADY-QL (5) was used to quantify the biogeochemical processes that lead to or result from the development of a reducing condition downgradient from landfill I. This program has been previously used to model the biogeochemical processes in a laboratory column (14). STEADYQL considers the system as a continuously stirred tank reactor (CSTR) by taking into

account flow through a single box, chemical speciation, and reaction kinetics. Knowledge of the average residence time, equilibrium constants, and reaction rate coefficients is required. The underlying assumption is that the inflow concentrations, reaction rates, and velocity are constant.

To model a flow-through system such as the one here, the region under study is subdivided into several reaches. Each reach is located between two wells and is treated as a CSTR, where the concentrations of species in the inflow and the outflow are known, and are used to determine zero-order reaction rate coefficients as described in the following section. Assuming a zero-order rate implies that, within each reach, the reaction rates are uniform. The true reaction rates may be of higher orders and dependent upon the concentrations of different substrates and the bacterial population and, as a result, are functions of the distance. Considering zero-order rates, however, does not affect the model output concentrations. The concentrations of the species that are used to calculate the rate coefficients (i.e., O_2 , NO_3^- , and Ca) are the independent variables. The dependent variables are the concentrations of those species whose turnover rates are directly or indirectly affected by all of the biogeochemical processes. In this study, DOC, DIC and pH are taken as the dependent variables. To examine the validity of our modeling assumptions, the simulated values of the dependent variables are compared to the field measurements.

Results and Discussion

Aqueous Phase. Concentrations of several relevant aqueous-phase species are shown in Table 1. The reported aqueous-phase data were collected and analyzed in March 1997. These data show small variation (<10%) from the data collected at different times between October 1995 and February 1997 for most redox-sensitive species (7).

Dissolved O_2 concentrations are below or close to the detection limit (3×10^{-6} M) under both landfills I and II (Table 1). In the downgradient direction from well 21, NO_3^- concentrations show an increase, while other species such as DOC, DIC, Ca, H_3BO_3 , SO_4 , and conductivity show a systematic decrease. Dissolved S(-II) is detected only under landfill I. Dissolved Fe(II) and Mn(II) are detected under both landfills. Concentrations of dissolved Fe(II) are the highest under landfill I, while dissolved Mn(II) concentrations remain relatively unchanged under both landfills.

The data reported in Table 1 represent the aqueous chemistry approximately at the top 2 m of the aquifer. The data for the deeper wells that extend down to a depth of ca. 6 m from the water table indicate lower concentrations of DOC, DIC, S(-II)_{aq}, Fe(II), Mn(II), H_3BO_3 , and Ca, lower conductivity, and a higher concentration of NO_3^- (7). Comparison of our measurements at different depths suggests that the leachate is mainly confined to the upper part of the aquifer, and any sinking of the plume must be within the top 2 m of the aquifer, equal to the height of the well screens.

The distribution of most of the species in Table 1 is directly or indirectly affected by microbially mediated redox processes. Under landfill I, low O_2 and NO_3^- concentrations together with the presence of NH_4^+ , S(-II)_{aq}, Fe(II), and Mn(II) indicate that microbially catalyzed aerobic respiration, denitrification/ NO_3^- reduction, Mn(III/IV), Fe(III), and SO_4 reduction reactions take place. The dominant processes at wells 22 and 23 downgradient from landfill I are the reduction of O_2 , NO_3^- and Mn(III/IV). It is not possible from our data to delineate precisely zones of different redox processes. However, it is expected that aerobic respiration takes place at the edge of the plume, followed by denitrification and Mn(III/IV) reduction.

Precipitation and Dissolution. An understanding of the saturation state with respect to the relevant solid phases is

TABLE 2. Aqueous-Phase Equilibrium Reactions

	log K ^a	ref
MgSO ₄ ⁰ ↔ Mg ²⁺ + SO ₄ ²⁻	-2.23	15
MgHCO ₃ ⁺ ↔ Mg ²⁺ + H ⁺ + CO ₃ ²⁻	-11.28	15
CaSO ₄ ⁰ ↔ Ca ²⁺ + SO ₄ ²⁻	-2.31	15
CaHCO ₃ ⁺ ↔ Ca ²⁺ + H ⁺ + CO ₃ ²⁻	-11.59	16
MnCO ₃ ⁰ ↔ Mn ²⁺ + CO ₃ ²⁻	-4.10	17
MnHCO ₃ ⁺ ↔ Mn ²⁺ + H ⁺ + CO ₃ ²⁻	-12.28	17
FeCO ₃ ⁰ ↔ Fe ²⁺ + CO ₃ ²⁻	-4.73	17
FeHCO ₃ ⁺ ↔ Fe ²⁺ + H ⁺ + CO ₃ ²⁻	-12.50	17
HCO ₃ ⁻ ↔ H ⁺ + CO ₃ ²⁻	-10.33	16
H ₂ CO ₃ ⁻ ↔ 2H ⁺ + CO ₃ ²⁻	-16.68	16
H ₂ S ↔ H ⁺ + HS ⁻	-6.90	15

^a Equilibrium constants for I = 0 M and 25 °C.

necessary for the geochemical characterization of an aquifer. This requires knowledge of the equilibrium solution speciation. Equilibrium speciation in solution was calculated from the aqueous phase data (Table 1) and the relevant equilibrium reactions listed in Table 2. Speciation calculations were performed after adjusting the equilibrium constants for the corresponding temperatures (Table 1) using v'ant Hoff equation and ionic strengths using Davies formula. The ionic strengths are 0.025, 0.018, 0.015, and 0.012 M for landfill I, well 22, well 23, and the oxic aquifer, respectively. The speciation data was then used to estimate the saturation conditions of different minerals, given the solubility limits of these minerals. The saturation state with respect to a mineral phase is commonly expressed in terms of the saturation index, SI:

$$SI = \log \frac{IAP}{K_s} \quad (1)$$

where IAP is the ion activity product for the mineral–water reaction and K_s is the equilibrium solubility product. A list of minerals relevant to this study and their corresponding values of K_s (25 °C) and SI (corrected for temperature) is given in Table 3.

Field measurements and equilibrium speciation calculations indicate that, in the oxic aquifer, the solution is in equilibrium with respect to calcite (SI = 0.00). The SI values for calcite increase slightly upgradient along the leachate plume (Table 3). The solution is, however, oversaturated with respect to dolomite (SI > 0) in all of the wells. Therefore, we have considered calcite precipitation and dilution as the most important mechanisms for the removal of Ca from the leachate.

TABLE 3. Solubility Relationships for Different Mineral Phases

	log K _s ^a	ref	SI ^b = log(IAP/K _s)					Oxic
			well 1	well 20	well 21	well 22	well 23	
calcite: CaCO ₃ (s) ↔ Ca ²⁺ + CO ₃ ²⁻	-8.480	(18)	0.37	0.15	0.19	0.19	0.01	0.00
dolomite: CaMg(CO ₃) ₂ (s) ↔ Ca ²⁺ + Mg ²⁺ + 2CO ₃ ²⁻	-17.09	(18)	2.68	1.92	1.70	1.49	1.08	1.00
magnesite: MgCO ₃ (s) ↔ Mg ²⁺ + CO ₃ ²⁻	-7.46	(19)	-0.67	-1.21	-1.46	-1.41	-1.49	-1.42
gypsum: CaSO ₄ (s) ↔ Ca ²⁺ + SO ₄ ²⁻	-4.58	(18)	-1.72	-1.59	-1.30	-1.50	-1.62	-2.01
rhodocrocite: MnCO ₃ (s) ↔ Mn ²⁺ + CO ₃ ²⁻								
crystalline	-11.13	(18)	0.51	0.26	0.21	0.39	0.03	c
synthetic	-10.39	(18)	-0.23	-0.48	-0.53	-0.35	-0.71	c
siderite: FeCO ₃ (s) ↔ Fe ²⁺ + CO ₃ ²⁻								
crystalline	-10.89	(18)	1.26	0.26	1.34	-0.79	-1.67	c
precipitated	-10.45	(18)	0.82	-0.18	0.90	-1.23	-2.11	c
amorphous FeS: FeS(s) + H ⁺ ↔ Fe ²⁺ + HS ⁻	-2.95	(20)	-0.28	-1.68	-0.36	c	c	c

^a Equilibrium constants for I = 0 M and 25 °C. ^b Corrected for the corresponding ionic strengths using Davies' formula and for the temperatures listed in Table 1 using V'ant Hoff equation. The solubility calculations for magnesite and amorphous FeS are carried out at 25 °C because of the lack of reaction enthalpy values for these minerals. The reaction enthalpies for precipitated siderite and synthetic rhodocrocite are assumed to be equal to their corresponding values for the crystalline minerals. ^c Very small IAP values. Solution is highly undersaturated. ^d Calculated for the sulfate-reducing wells only.

The solution throughout the study area is undersaturated with respect to magnesite (SI < 0). Downgradient from landfill I, the Mg concentrations remain relatively constant (Table 1). Higher Mg concentration under the landfill I is due to the solid waste and is subject to dilution in the downgradient direction without taking part in any reactions.

As indicated in Table 3, the groundwater system is undersaturated with respect to gypsum (SI = -1.30 to -2.01). The excess concentration of SO₄ under landfill I possibly originates from the solid waste.

Manganese is detected in the aqueous phase at 10 to 20 μM concentrations under both landfills (Table 1). Unlike other redox indicators, dissolved Mn(II) concentrations are similar in all wells. Besides Mn-reducing bacteria, Fe(II), S(-II)_{aq}, and reactive organic matter can reduce the oxidized Mn species. Under landfill II in wells 22 and 23, however, where negligible concentrations of dissolved Fe(II) and S(-II) are detected, microbially catalyzed reduction is an important process in Mn(III/IV) dissolution. The presence of Mn(II) in wells 22 and 23 may also be partly attributed to transport from upgradient. Under anoxic conditions and in the presence of sufficient alkalinity, precipitation and adsorption are the most important mechanisms for the removal of Mn(II). Solubility calculations (Table 3) show that under the anoxic conditions, concentrations of dissolved Mn are in near-equilibrium with rhodocrocite [MnCO₃(s)]. The SI values reported with respect to the crystalline and the synthetic MnCO₃(s) range between 0.03 and 0.51 and -0.71 to -0.23, respectively. Given the uncertainties in the reported solubility constants, such slight deviations are within the acceptable limits of equilibrium conditions. Therefore, Mn(II) concentration along the leachate plume is most probably regulated by precipitation as MnCO₃(s).

Solubility calculations show that directly under landfill I, precipitation of siderite [FeCO₃(s)] would be possible (Table 3). At the three wells under landfill I, the SI values with respect to crystalline siderite are positive. Oversaturation with respect to precipitated siderite is observed at wells 1 and 21, suggesting that precipitation of siderite is a kinetically controlled process.

A near-equilibrium condition with respect to the solubility of amorphous FeS at wells 1 and 21 is estimated (Table 3), suggesting that Fe(II) concentrations at these wells are controlled by the solubility of FeS. Downgradient from landfill I, Fe(II) is undersaturated with respect to both minerals.

Geochemical Modeling of the Aqueous Phase. For modeling purposes with STEADYQL, the aquifer in this study

TABLE 4. Kinetically Controlled Geochemical Processes

processes	stoichiometry	rate coefficients (M s ⁻¹)		
		well 21-well 22	well 22-well 23	eq
aerobic respiration	CH ₂ O + O ₂ → H ⁺ + HCO ₃ ⁻	7.2 × 10 ⁻¹²	3.3 × 10 ⁻¹²	2
denitrification	5CH ₂ O + 4NO ₃ ⁻ + 4H ⁺ → 2N ₂ + 5CO ₂ + 7H ₂ O	2.8 × 10 ⁻¹²	3.9 × 10 ⁻¹³	3
Mn(IV) reduction	CH ₂ O + 2MnO ₂ + H ₂ O → 2Mn ²⁺ + 3OH ⁻ + HCO ₃ ⁻			4
Fe(III) reduction	CH ₂ O + 4FeOOH + 2H ₂ O → 4Fe ²⁺ + 8OH ⁻ + H ₂ CO ₃			5
SO ₄ reduction	2CH ₂ O + SO ₄ ²⁻ → HS ⁻ + H ⁺ + 2HCO ₃ ⁻			6
CaCO ₃ precipitation	Ca ²⁺ + CO ₃ ²⁻ → CaCO ₃ (s)	3.3 × 10 ⁻¹¹	1.6 × 10 ⁻¹¹	7

is subdivided into two reaches: (1) from well 21 to well 22 and (2) from well 22 to well 23 (Figure 1). We have assumed that the aquifer under study is homogeneous with respect to the flow velocity and that wells 21, 22, and 23 are situated on the same flow line (i.e., a one-dimensional flow field is considered). The measured concentrations of the aqueous-phase species at wells 21 and 22 have been used as the inflow concentrations for well 21–well 22 and well 22–well 23 reaches, respectively. The model takes into account dilution from the adjacent oxic aquifer, but considers no contribution from landfill II where wells 22 and 23 are located (Figure 1). The vertical mixing of the leachate has also been assumed to be negligible.

The kinetically controlled processes that influence the biogeochemical changes and their corresponding rate coefficients for each reach are depicted by eqs 2–7 (Table 4). These processes were chosen based upon our aqueous-phase measurements (Table 1). The rate coefficients listed in Table 4 are zero-order and are estimated by the change in concentrations of the corresponding aqueous species within each reach after taking into the account the effect of dilution and the average velocity. Dilution may be an important factor that influences the concentrations of various species in a leachate plume. In this study, H₃BO₃ is used as a conservative tracer to characterize the study area with respect to dilution. Average H₃BO₃ concentrations measured at the upper 2 m of the groundwater gradually diminish in the downgradient direction along the leachate plume (Table 1). Chloride concentrations do not exhibit a systematic decrease from wells 21 to 23. The fluctuating concentration of Cl⁻ in the downgradient direction may possibly be due to leaching from landfill II. Therefore, Cl⁻ has not been used as the conservative tracer. The dilution factor at each well is estimated by evaluating the effect of the background H₃BO₃ concentration in the oxic aquifer and that of well 21 on wells 22 and 23 as follows (21):

$$[H_3BO_3]_{\text{well}22} = x[H_3BO_3]_{\text{well}21} + (1 - x)[H_3BO_3]_{\text{oxic}} \quad (8)$$

where, *x* is the fraction of water originating from landfill I. For well 22, *x* = 0.54, and for well 23, *x* = 0.28.

The rate coefficients are estimated as described below for aerobic respiration, denitrification, and calcite precipitation processes (eqs 2, 3, and 7). Precipitation of calcite is considered as a kinetically controlled process (eq 7), since as discussed above, our measurements indicate that under both landfills I and II the leachate is oversaturated with respect to calcite. Aqueous concentrations of dissolved O₂, NO₃⁻, and Ca are used as independent variables to estimate the rate coefficients for eqs 2, 3, and 7, respectively. Dissolved inorganic carbon, DOC, and pH are the dependent variables, since their turnover rates depend on these rate coefficients. Therefore, to examine the validity of our assumptions, the modeled values for the dependent variables are compared to the field measurements in the following section.

The rate coefficients listed in Table 4 are calculated after correcting for dilution as illustrated here for the denitrification process for the reach between wells 21 and 22: nitrate concentrations for wells 21, 22, and the oxic aquifer are listed in Table 1. If mixing with the oxic aquifer were the only process leading to the increase in NO₃⁻ concentration in the downgradient direction, then according to eq 8, the NO₃⁻ concentration at well 22 would be 310 μM. However, the measured concentration at this well is 180 μM (Table 1). Therefore, 130 μM of NO₃⁻ has been microbially reduced in this reach. Dividing this number by an average residence time of 1.15 × 10⁷ s between wells 21 and 22 and a stoichiometric factor of 4 (eq 3) gives us a zero-order rate coefficient of 2.8 × 10⁻¹² M s⁻¹ for the denitrification process (Table 4).

Ammonium is detected throughout the anoxic part of the aquifer (Table 1). Ammonium under landfill I may be released from the organic matter or may be due to the process of microbially catalyzed NO₃⁻ reduction. The disappearance of NH₄⁺ outside of landfill I may be attributed to dilution, as well as ion exchange and adsorption (22), and possibly oxidation.

The rate of aerobic respiration is estimated by equating it to the rate of dilution of dissolved O₂ into the anoxic leachate from the adjacent oxic aquifer. Aerobic respiration takes place primarily at the periphery of the plume, but its effect on the concentration of the dependent variables has been considered in a one-dimensional sense.

Dissolved S(-II) measurements at wells 1, 20, and 21 indicate the presence of SO₄-reducing zones under landfill I (Table 1). At well 22, however, S(-II)(aq) concentration diminishes to below the detection limit, and the decrease in the concentration of SO₄ from wells 21 to 22 may be explained by dilution. Therefore, given the dilution factor used, the SO₄-reduction process contributes little to the turnover of DOC and DIC downgradient from landfill I and is neglected here. Sulfate reduction, however, cannot be strictly ruled out between wells 21 and 22, as this process may take place at the proximity of landfill I, between wells 21 and 22. Outside of landfill I, SO₄ reduction rate is limited by the availability of DOC.

Estimation of Mn(III/IV) and Fe(III) reduction rates independently from our data is not possible, since Mn(II) and Fe(II) species are subject to precipitation and adsorption. Furthermore, due to the relatively low concentrations of dissolved Mn and Fe downgradient from landfill I, the reduction processes depicted by eqs 4 and 5 do not contribute significantly to changes in the DOC and DIC concentrations and have been neglected. However, a knowledge of the rates of production, precipitation, and reaction of Fe(II) and Mn(-II) species remains very important in understanding the distribution of many trace metals and organic contaminants.

STEADYQL Simulation Results. Measured and modeled values of the dependent variables DOC, DIC, and pH and the

TABLE 5. STEADYQL Simulation Results

location	DOC (ppm)		DIC (mM)		pH	
	measured	modeled	measured	modeled	measured	modeled
well 22	5.3	7.2	11.0	12.4	6.76	6.77
well 23	2.3	2.8	8.8	9.5	6.90	6.77

processes	Sensitivity Analysis					
	$\frac{\partial \ln[\text{DOC}]}{\partial \ln k}$		$\frac{\partial \ln[\text{DIC}]}{\partial \ln k}$		$\frac{\partial \ln[\text{H}^+]}{\partial \ln k}$	
	well 22	well 23	well 22	well 23	well 22	well 23
aerobic respiration	-9.5×10^{-2}	-2.5×10^{-1}	4×10^{-3}	5×10^{-3}	1.8×10^{-2}	2.4×10^{-2}
denitrification	-1.9×10^{-1}	-1.5×10^{-1}	9×10^{-3}	4×10^{-3}	$<10^{-3}$	$<10^{-3}$
calcite precipitation	0	0	-2.1×10^{-2}	-3.0×10^{-2}	1.2×10^{-1}	1.7×10^{-1}
dilution	-2.6×10^{-1}	-1.9×10^{-1}	-1.3×10^{-1}	-8.0×10^{-2}	-2.3×10^{-1}	-2.1×10^{-1}

normalized sensitivity coefficients are listed in Table 5. The processes listed in Table 4 directly affect the concentrations of these variables, and therefore, a comparison between the field measurements and the simulation results for these values provides a standard to verify the validity of our model assumptions.

The agreement between the measured and the modeled data in Table 5 indicates that STEADYQL simulation results for DOC, DIC, and pH in wells 22 and 23 are reasonable, if one considers the underlying modeling assumptions and the uncertainties in the measurements. The factors that influence the simulation results are the reaction rate (Table 4), the dilution rate, and the input concentration of species for each reach. It is difficult to investigate the influence of each of these factors independently, as the former two are dependent upon the latter.

Sensitivity analysis with respect to the parameters that control the concentrations of the dependent variables is a useful way to study the influence of each parameter on chemical speciation. The program STEADYQL quantifies the effect of all of the parameters on all of the components. The normalized sensitivity coefficients for each component such as DOC, DIC, and H⁺ are calculated as follows:

$$\frac{\partial \ln X}{\partial \ln k} = \sum_i \alpha_i \frac{\partial \ln c_i}{\partial \ln k} = \sum_i \alpha_i \frac{\partial c_i}{\partial k} \frac{k}{c_i} \quad (9)$$

where, c_i is the concentration of species i forming the component X such that $X = \sum_i c_i$, k is the rate coefficient for a given process, and α_i is the concentration fraction of species i . The values of the normalized sensitivity coefficients for the components DOC, DIC, and pH with respect to several processes are presented in Table 5. These values signify the percent change in the modeled concentrations for a 1% change in the corresponding rate coefficients (14). Negative and positive signs indicate processes that lead to the consumption and production of the dependent variables, respectively.

The processes considered here, with the exception of calcite precipitation, lead to the decrease of DOC. For the reach between wells 21 and 22, the sensitivity coefficients in Table 5 show that the redox processes and dilution contribute approximately equally to the disappearance of DOC, while for the reach between wells 22 and 23, the redox processes are more important than dilution.

According to Table 5, aerobic respiration and denitrification are almost equally important for the consumption of DOC. An increase in the rate of any of these two processes would result in a decrease in DOC concentration downgradient.

The modeled values listed in Table 5 are valid for the given reaction stoichiometries in Table 4. For the redox

reactions (eqs 2 and 3), these stoichiometries are a function of the oxidation state of the organic electron donor. We have considered CH₂O, with an oxidation state of zero, as the electron donor for the aerobic respiration and denitrification. Lower oxidation states of DOC would cause higher consumption rates of the organic matter for a given reaction rate coefficient.

The normalized sensitivity coefficients for the redox processes in Table 5 are positive with respect to the DIC concentration, indicating production of DIC (eqs 2 and 3). Precipitation of calcite and dilution, however, lead to the consumption of DIC, and their coefficients have negative signs. The absolute values of these coefficients suggest that, for both reaches in this study, dilution followed by calcite precipitation processes are more important than the redox processes in controlling the DIC. Dilution and calcite precipitation are more important in controlling the pH than the redox processes.

Reducing the dilution factor $1 - x$ (eq 8) between wells 21 and 22 by one-half results in a simulated DIC concentration of 12.7 mM and a DOC concentration of 8.1 ppm in well 22. The relative lack of sensitivity to dilution, despite high values of the normalized sensitivity coefficients with respect to dilution (Table 5), is due to the dependence of the reaction rates on the dilution factor. A decrease in dilution causes a decrease in the aerobic respiration and the denitrification rates and an increase in the rate of calcite precipitation.

The most important assumption invoked in the model is that the aquifer system is geochemically and hydrologically homogeneous. This implies that in a given reach, the rates of reaction and dilution do not vary. One way to curtail the uncertainty regarding such assumptions is to drill additional sampling wells at locations where high dilution or transformation rates are expected. At the site studied here, additional wells between the existing wells 21 and 22 where the estimated dilution rate is high would provide more insight into the processes involved.

Solid Phase. In reduced sediments, the solid phase usually contains considerably higher concentrations of electron donor and electron acceptor species than the aqueous phase (23). This has significant long-term implications on the behavior of an aquifer in the event that extreme oxidizing (e.g., aquifer oxygenation) or reducing (e.g., introduction of oxidizable organic matter) conditions are introduced. The OXC of an aquifer is defined as its ability to restrict the migration of a reduced plume, whereas the reduction capacity (TRC) of an aquifer is its ability to control the extent of an oxidizing condition (12, 23). Oxidation and reduction capacities are defined operationally as the equivalent concentrations of Ti(III)-reducible (12) and K₂Cr₂O₇-oxidizable (23) compounds, respectively. In their study of a solid waste landfill leachate plume, Heron et al. (10, 12, 24) discovered that iron(III) oxides provide the largest pool of

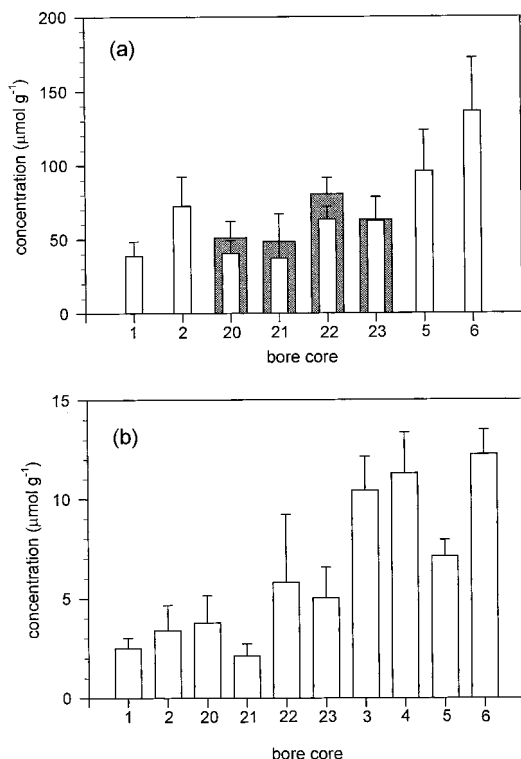


FIGURE 2. (a) Concentration of Fe(III) extracted by Ti(III)-EDTA for different cores (white columns). Concentration of oxidized Ti(III) for different cores (cross-hatched columns). (b) Fe(III) concentration extracted using the ascorbate technique. The error bars represent 1 standard deviation from at least six measurements along a 2 m depth.

electron-accepting species. Even though solid-bound organic matter seems to have a significant effect on the TRC, solid Fe(II) and sulfides correlate with the TRC (24). The use of OXC and TRC indices to estimate the response of a reduced aquifer to reducing and oxidizing conditions is limited by the fact that the true redox buffering capacity of a system is kinetically controlled. In this study, we have used chemical extraction techniques to characterize the solid-phase species that are of potential importance in electron-transfer reactions in the aquifer system.

The distribution of the total Ti(III)-reducible Fe(III) in the aquifer system is shown in Figure 2a. The cores under landfills I and II have smaller average Fe(III) concentrations than those from the oxic wells. Relatively low Fe(III) concentrations under landfill I are due to reductive dissolution of iron(III) (hydr)oxides. Under landfill I, this process is carried out enzymatically by the Fe(III)-reducing bacteria (eq 5) and nonenzymatically by dissolved S(-II) (25). Presence of Fe(III)-reducing bacteria in this aquifer system has been shown in a separate laboratory column study (26). Despite the fact that Fe(III) reduction at wells 22 and 23 is not presently expected, cores collected from these wells indicate smaller concentrations of Fe(III) than cores collected from the oxic aquifer. This observation sheds light on the past activity of the aquifer system. Low Fe(III) concentrations at wells 22 and 23 may be due to the previous Fe(III)-reducing activity of landfill II. Alternatively, reduction of Fe(III) may have taken place in the past along the leachate plume of landfill I, when higher concentrations of the DOC permitted Fe(III)-reducing activities downgradient.

Shown in Figure 2a as crosshatched columns are the concentrations of the oxidized Ti(III) in cores 20-23. For these cores, Fe(III) is the most important electron acceptor, as its reduction to Fe(II) accounts for more than 80% of the

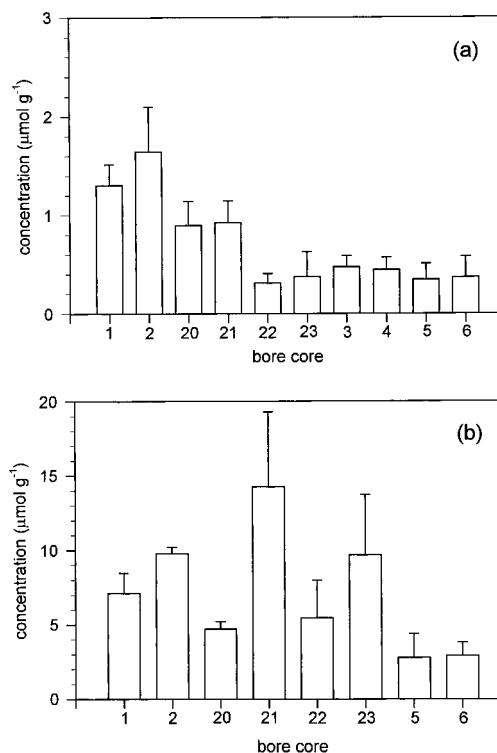


FIGURE 3. Concentration of sulfur in the (a) acid-volatile sulfide and (b) Cr(II)-HCl extraction experiments for different cores. The error bars represent one standard deviation from at least six measurements along a 2 m depth.

oxidation of Ti(III). The OXC values obtained from the oxidation of Ti(III) range between 50 and 80 $\mu\text{equiv g}^{-1}$ and are similar to the values reported by Heron and Christensen (24) for the anoxic conditions in the Vejen landfill, Denmark. In our aquifer system, an OXC of 100-150 $\mu\text{equiv g}^{-1}$ is expected in the oxic soil (Figure 2a). Therefore, an approximate 50% loss in the OXC is observed in the anoxic soils, underscoring the importance of solid Fe(III) as an electron acceptor.

The ascorbate-extractable Fe(III) concentrations for different cores are shown in Figure 2b. The average concentration of the amorphous iron(III) (hydr)oxide under landfill I is 3.0 $\mu\text{mol g}^{-1}$. This concentration increases to 5.4 $\mu\text{mol g}^{-1}$ downgradient in wells 22 and 23, where anoxic conditions prevail, and to 10.3 $\mu\text{mol g}^{-1}$ in the oxic aquifer soil. Amorphous Fe(III) (hydr)oxide is the most reactive Fe(III) solid phase with respect to enzymatic (27) and nonenzymatic reductive dissolution processes (25, 28). Even though the average weight-normalized concentrations of amorphous iron(III) (hydr)oxide are approximately 10% of the total Fe(III), the former phase possesses significantly larger surface area than the latter, due to the higher specific surface area of amorphous phase than crystalline phases of iron(III) (hydr)oxides (29).

The AVS measurements of the solid samples are shown in Figure 3a. These measurements indicate the amorphous FeS concentration primarily. The cores under landfill I clearly show higher values of AVS than other cores. This is attributed to the presence of SO_4 -reducing conditions under this landfill. At this location, a near-saturation condition with respect to FeS exists (Table 3). Downgradient in wells 22 and 23 where no SO_4 -reducing activity is observed, the solution is highly undersaturated with respect to FeS (Table 3), and the AVS concentration at these bore cores diminishes to the background level of ca. 0.5 $\mu\text{mol g}^{-1}$ that is observed also in the oxic cores. Given that the amorphous FeS oxidizes readily in the presence of dissolved O_2 , the background AVS in the

oxic soils must be from within the calcite deposit.

The results for the Cr(II)–HCl extraction of the bore cores are shown in Figure 3b. This method allows the extraction of the total reducible sulfur in the soil, consisting mainly of FeS, FeS₂ (pyrite), and elemental and organic S. The concentration of acetone-extracted elemental and organic S is between 0.2 and 0.5 μmol g⁻¹ in the anoxic region (results not shown here). From Figure 3a, the average FeS concentration is less than 20% of the total sulfur. Therefore, Figure 3b shows primarily the concentration of FeS₂. Distribution of FeS₂ in the anoxic region of the aquifer studied here does not show any systematic trend. The presence of FeS₂ at bore cores 22 and 23, where SO₄-reducing condition does not presently exist, is another indicator that this process has been active under landfill II in the past.

The contribution of the solid Fe(II) and sulfur species to the theoretical TRC may be written as [Fe(II)] + 8[S(-II)] + 7[S(-I)] + 6[S(0)]. For cores 1, 2, 20, and 21, a TRC value of 80 μequiv g⁻¹ is estimated. The estimated TRC for wells 22 and 23 is 53 μequiv g⁻¹. These values are similar to the lower end of the measured TRC values reported by Heron and Christensen (24) for an anaerobic sandy aquifer.

Oxidation and reduction capacities of an aquifer have long-term implications. The OXC and TRC reported here are the limiting values that are estimated without considering the role of redox kinetics. The surface-area-normalized dissolution rate of different iron(III) (hydr)oxide phases by dissolved S(-II) exhibited 1 order of magnitude difference between lepidocrocite and hematite (25). Similarly, kinetics of oxidation of sulfur species would be faster for amorphous FeS than for FeS₂. Redox kinetics of the solid-phase plays an important role in the response of an aquifer to extreme oxidizing or reducing conditions, and its knowledge is essential for the planning of remediation schemes.

Conclusions

In this paper, the aqueous- and solid-phase biogeochemistry of a municipal solid waste landfill were studied. Microbially catalyzed reaction kinetics and the dilution process down-gradient from a municipal landfill were quantified, and with the aid of a geochemical model, STEADYQL, the relative importance of each process was elucidated. Dilution seemed to be the most important process in the attenuation of the organic matter. Due to the relatively low concentration of DOC presently leaving landfill I, anaerobic processes such as Fe(III) and SO₄ reductions do not take place outside of this landfill. This is partially due to the fact that the landfill was capped in 1963 and is relatively old. Solid-phase extractions of the aquifer material outside of landfill I in the anoxic zone (wells 22 and 23), however, indicate reduction of the OXC and an increase of the TRC values relative to the oxic aquifer, suggesting the existence of Fe and SO₄ reducing environments in the past.

Acknowledgments

Drs. Eduard Hoehn, Peter Huggenberger, and Jürg Zobrist were involved in the planning and execution of the project. Thanks go to Hans-Rudolf Zweifel, Thomas Rüttimann, Dr. Adrian Ammann, Martin Bühlmann, Kathrin Tschannen, and Suzanne Mettler who helped to organize and assisted in sample collection and analysis. Dr. Gerhard Furrer is acknowledged for his help with STEADYQL program. Profes-

sor Werner Stumm and Drs. Jürg Zobrist and Urs von Gunten are thanked for many discussions and for reviewing the manuscript. The careful review of two anonymous reviewers is greatly appreciated.

Literature Cited

- (1) Bjerg, P. L.; Rügge, K.; Pedersen, J. K.; Christensen, T. H. *Environ. Sci. Technol.* **1995**, *29*, 1387–1394.
- (2) Chapelle, F. H.; Zelibor, J. L.; Grimes, D. J.; Knobel, L. L. *Water Resour. Res.* **1987**, *23*, 1625–1632.
- (3) Jacobs, L. A.; von Gunten, H. R.; Keil, R.; Kuslys, M. *Geochim. Cosmochim. Acta* **1988**, *52*, 2693–2706.
- (4) von Gunten, U.; Zobrist, J. *Geochim. Cosmochim. Acta* **1993**, *57*, 3895–3906.
- (5) Furrer, G.; Westall, J.; Sollins, P. *Geochim. Cosmochim. Acta* **1989**, *53*, 595–601.
- (6) Abbaspour, K.; Matta, V.; Huggenberger, P.; Johnson, C. A. *J. Contam. Hydrol.* **1998**, submitted for publication.
- (7) Zweifel, H. R.; Ulrich, A.; Ammann, A., *Chemische Untersuchungen von vier Altlasten in Winterthur Riet*, EAWAG: Dübendorf, Switzerland, 1997.
- (8) Hoehn, E.; Honold, P. *Schweiz. Ing. Arch.* **1998**, submitted for publication.
- (9) Zhabina, N. N.; Volkov, I. I. In *Environmental Biogeochemistry: Methods, Metals and Assessments*; Krumbein, W. E., Ed.; Ann Arbor Science Publishers: Ann Arbor, MI, 1978; pp 735–745.
- (10) Heron, G.; Crouzet, C.; Bourg, A. C. M.; Christensen, T. H. *Environ. Sci. Technol.* **1994**, *28*, 1698–1705.
- (11) Kostka, J. E.; Luther, G. W., III. *Geochim. Cosmochim. Acta* **1994**, *58*, 1701–1710.
- (12) Heron, G.; Christensen, T. H.; Tjell, J. C. *Environ. Sci. Technol.* **1994**, *28*, 153–158.
- (13) Canfield, D. E.; Raiswell, R.; Westrich, J. T.; Reaves, C. M.; Berner, R. A. *Chem. Geol.* **1986**, *54*, 149–155.
- (14) Furrer, G.; von Gunten, U.; Zobrist, J. *Chem. Geol.* **1996**, *133*, 15–28.
- (15) Martell, A. E.; Smith, R. M. *Critical Stability Constants, Vol. 5: First Supplement*; Plenum: New York, 1982.
- (16) Smith, R. M.; Martell, A. E. *Critical Stability Constants, Vol. 6: Second Supplement*; Plenum: New York, 1989.
- (17) Fouillac, C.; Criaud, A. *Geochem. J.* **1984**, *18*, 297–330.
- (18) Nordstrom, D. K.; Plummer, L. N.; Langmuir, D.; Busenberg, E.; Hay, H. M.; Jones, B. F.; Parkhurst, D. L. In *Chemical Modeling of Aqueous Systems II*; Melchior, D. C.; Bassett, R. L., Eds.; ACS Ser. 416, American Chemical Society: Washington, DC, 1990; pp 398–413.
- (19) Smith, R. M.; Martell, A. E. *Critical Stability Constants: Inorganic Complexes*; Plenum: New York, 1976; Vol. 4.
- (20) Davison, W. *Aquat. Sci.* **1991**, *53*, 309–329.
- (21) Bourg, A.; Bertin, C. *Environ. Sci. Technol.* **1993**, *27*, 661–666.
- (22) Doussan, C.; Poitevin, G. P.; Ledoux, E.; Detay, M. *J. Contam. Hydrol.* **1997**, *25*, 129–156.
- (23) Barcelona, M. J.; Holm, T. R. *Environ. Sci. Technol.* **1991**, *25*, 1565–1572.
- (24) Heron, G.; Christensen, T. H. *Environ. Sci. Technol.* **1995**, *29*, 187–192.
- (25) dos Santos Afonso, M.; Stumm, W. *Langmuir* **1992**, *8*, 1671–1675.
- (26) Amirbahman et al. Manuscript in preparation.
- (27) Lovely, D. R.; Phillips, E. J. P.; Lonergan, D. J. *Environ. Sci. Technol.* **1991**, *25*, 1062–1067.
- (28) Amirbahman, A.; Sigg, L.; von Gunten, U. *J. Colloid Interface Sci.* **1997**, *194*, 194–206.
- (29) Cornell, R. M.; Schwertmann, U. *The Iron Oxides: Structure, Properties, Reactions, Occurrence and Uses*; VCH: Weinheim, Germany, 1996.

Received for review September 10, 1997. Revised manuscript received March 18, 1998. Accepted April 7, 1998.

ES970810J